

Quantification of freezing-induced damage in reinforced concrete

K. Zandi Hanjari

Dep. of Civil and Environmental Engineering, Chalmers University of Technology, Göteborg, Sweden

P. Kettil

Dep. of Applied Mechanics, Chalmers University of Technology, Göteborg, Sweden

K. Lundgren

Dep. of Civil and Environmental Engineering, Chalmers University of Technology, Göteborg, Sweden

ABSTRACT: The paper presents a methodology to analyze the mechanical behavior of reinforced concrete structures with an observed amount of freezing-damage at a given time. It is proposed that the effect of internal freezing damage can be modeled as change of material properties, and that surface scaling can be modeled as change in geometry. The change in material properties was examined, and it was found that relations between compressive and tensile strength commonly used for undamaged concrete could not be directly applied to freezing damaged concrete. A modified relation was suggested. The proposed methodology was tested on concrete beams affected by internal freezing damage, using non-linear finite element analyses based on fracture mechanics in the program Diana, and the results were compared with available experimental results. The results indicated that an uncertainty in the analyses was the Young's modulus for damaged concrete, and that this influenced the results to a rather large extent.

1 INTRODUCTION

There is a growing need for reliable methods of assessing deteriorated structures, since an optimized maintenance and repair method involves the capability to predict the load-carrying capacity and remaining service life of deteriorated structures. In an ongoing research project, load-carrying capacity of damaged bridges is studied on the structural and component level. Mainly damage due to environmental impacts will be considered, such as corrosion, damage due to freezing, splitting of covers, and damaged bond between the concrete and reinforcement. The part of the project presented here is mainly focused on damage due to freezing, which is one of the major causes of deterioration in reinforced concrete structures and is still a pending research topic in assessment of old bridges.

While previous research has been chiefly concerned with the causes and mechanisms of freezing deterioration, relatively little attention has been given to the problem of assessing the residual load-bearing capacity of deteriorated reinforced concrete structures. This has exposed the need for improved understanding of freezing damage effects upon structural integrity. The aim of this research is to develop a method to quantify the damage caused by freezing of reinforced concrete.

Freezing damage in concrete is caused by the volume expansion of freezing water in the concrete pore system. If the expansion cannot be accommo-

dated in the pore system, but is restrained by the surrounding concrete, it induces tensile stresses in the concrete. The tensile stresses cause cracks, which affect the strength, stiffness, and fracture energy of the concrete as well as the bond strength between the reinforcing bar and surrounding concrete in damaged regions; see Powerst (1945) and Shih (1988).

Two types of freezing damage can be distinguished, Fagerlund (2004):

1. Internal freezing damage caused by freezing of moisture inside the concrete. This may cause cracking and substantial reduction of strength and stiffness, Fagerlund (2004).

2. Surface scaling, which is usually caused by freezing of salt water in contact with the concrete surface. This damage usually results in spalling of the concrete surface, while the remaining concrete is mainly unaffected, Fagerlund (2004) and Gudmundsson (1999).

This paper presents a methodology to analyze the mechanical behavior (e.g. stiffness and strength) of reinforced concrete structures affected by freezing damage. At this stage, the methodology is restricted to the prediction of the mechanical behavior for a structure with an observed amount of damage at a given time. The freezing-damage development over time is not included.

The paper is organized as follows: Chapter 2 presents the proposed methodology. In Chapter 3, the methodology is tested on concrete beams affected by

internal freezing damage. Finally, Chapter 4 concludes the work.

2 MODELING OF FREEZING DAMAGE

In the following, a methodology to analyze the mechanical behavior of reinforced concrete structures affected by freezing damage is proposed. The methodology is based on the assumption that the usual method of structural analysis applies. Furthermore, it is assumed that the effect of internal freezing damage can be modeled as change of material properties; i.e. reduction of strength and stiffness, and that surface scaling can be modeled as change in geometry; i.e. reduction in dimensions.

2.1 Change of material properties

Internal freezing damage is here modeled as change of material properties; i.e. reduction of strength and stiffness.

2.1.1 Compressive strength

Measurements of the compressive strength for internal freezing damage have been reported in e.g. Fagerlund (1994). Internal frost-damage is caused by freezing of water inside the concrete. The damage caused by freezing is always extended to such parts of the concrete where the degree of water saturation, S , exceeds the critical value. The critical degree of saturation, S_c , is a material property and independent of the number of frost cycles and freezing rate. As reported in Fagerlund (1994), in order to reach different degree of saturation, certain fractions of air bubbles, captured inside the pore system of concrete during casting, had to be water-filled. This could only be achieved by dissolution of the entrapped air and replacement by water to different extent. Vacuum treatment to different residual pressure (of 2, 20, and 50 mm Hg), have been used to empty the initially air-filled pores in the concrete and make it possible for water to rapidly fill the pore system of concrete including the air pores.

So far, based on a study of the reported results, it seems not possible to directly relate the reduction of compressive strength to the extent of freezing damage observed. Hence, it must be concluded that at least the compressive strength must be measured in each individual case by e.g. compression tests on a few drilled cores, supplemented with non-destructive testing such as with Schmidt-hammer, to determine the extent of the damaged region.

2.1.2 Other strength and stiffness properties

For undamaged concrete, relations between compressive strength and other properties such as tensile strength, stiffness, and fracture energy are well established and widely used. For practical reasons, to reduce the required amount of testing down to com-

pressive tests only, it would be useful if similar relations could be found for freezing damaged concrete. Therefore, in Figure 1 test results for tensile strength and Young's modulus for freezing damaged concrete are compiled and plotted versus measured damaged compressive strength. This is compared with relations for and test results of undamaged concrete.

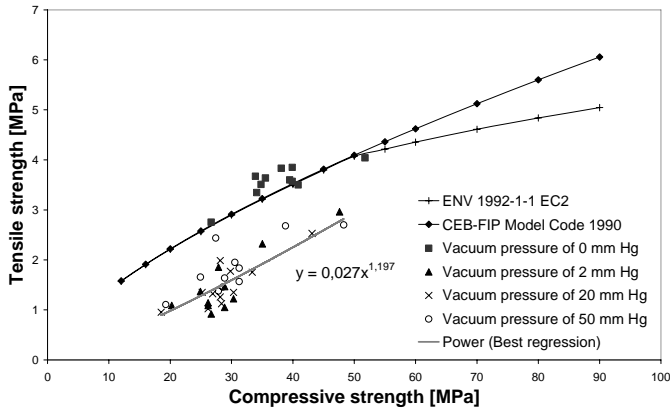
All test results are from Fagerlund (1994). It should be noted that the tests of the compressive strength have been done on three specimens for each case. The measured compressive strengths were recalculated from 100 mm cube to 150 mm cube by multiplying with a factor of 0.96, according to Neville (2003), and then to standard 150*300 mm cylinder that commonly are used in different codes according to Ljungkrantz *et al.* (1994). The tensile strengths were obtained from measured splitting tensile strength by multiplying with a factor of 0.9 according to CEB (1993). Finally, Young's modulus was obtained from dynamically measured Young's modulus, reported by Fagerlund (1994), by multiplying with a factor of 0.83, according to Neville (2003).

As can be seen in Figure 1, the relations for undamaged concrete cannot be used directly for freezing damaged concrete. The tensile strength of the damaged concrete is markedly lower than would be estimated from the relations for undamaged concrete. By curve fitting, although the scatter is large, the following relation for damaged concrete is suggested:

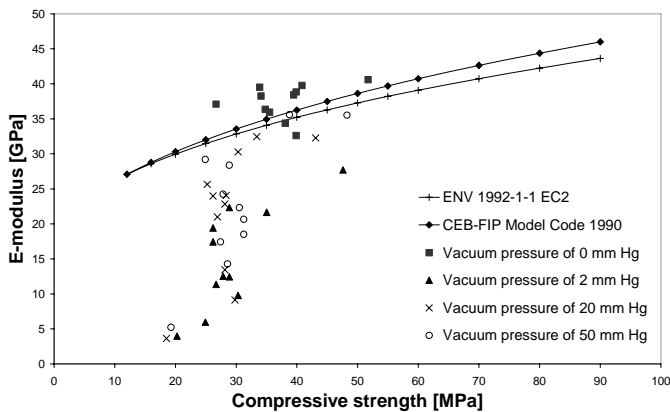
$$f_{ct} = 0.027 f_{cc}^{(1.197)} \quad (1)$$

where f_{ct} is the tensile strength of the damaged concrete and f_{cc} is the measured compressive strength of concrete using standard 150*300 mm cylinder. The suggested relation is also shown in Figure 1.

For Young's modulus, the results are unclear; while many results indicate lower values than would be expected from the relations for undamaged concrete, some even indicate higher values. Due to this large scatter, it was not considered possible to give any suggested relation between compressive strength and Young's modulus.



(a)



(b)

Figure 1. Relations between (a) compressive strength and tensile strength, and (b) compressive strength and Young's modulus for undamaged and freezing damaged concrete; test results from Fagerlund (1994).

2.1.3 Stress-strain curve and failure envelope

In absence of experimental investigations, the only, but yet reasonable, possibility is to assume that the shapes of the stress-strain relation and failure envelope of the freezing damaged concrete are the same as for undamaged concrete.

2.2 Change of geometry

Surface scaling freezing damage is suggested to be modeled as change of geometry; i.e. reduction in dimensions. The remaining concrete is assumed to be unaffected, according to Gudmundsson (1999). The extent of the damaged region and the depth of surface scaling must be measured on site. The geometry of the structural analysis model must be updated accordingly.

3 FE ANALYSIS - COMPARISON WITH TESTS

In the following, the methodology proposed in Chapter 2 was tested on concrete beams affected by

internal freezing damage. No tests on the structural effects of scaling damage were found in the literature; therefore no such comparisons could be done.

3.1 Experimental test setup

Four-point bending tests of frost damaged reinforced concrete were reported by Hassanzadeh (2006). A short summary of the test setup relevant for the finite element (FE) analysis is given in the following.

In total 14 beam tests have been carried out, comprising two different geometries, varying reinforcement content (bending reinforcement content ratio $\omega/\omega_b = 64 - 114\%$, and with and without stirrups), and different climate exposure (L = laboratory climate, S and V varying forms of freezing exposure). In addition, the compressive strength, splitting tensile strength and fracture energy have been measured on cubes, cylinders and RILEM test beams. The compressive and tensile strength of the concrete exposed to freezing have been determined from cores drilled out from concrete blocks stored in the same conditions as the beams. The specimens exposed to freezing showed typical internal freezing damages. Surface scaling did not occur.

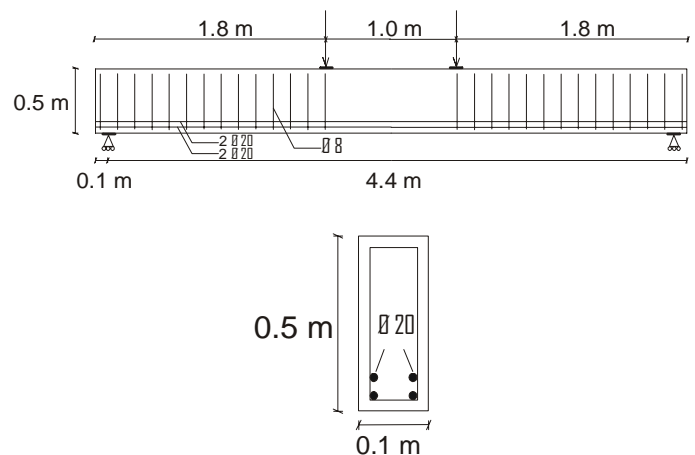


Figure 2. Example of geometry of beams tested, redrawn from Hassanzadeh (2006).

3.2 Finite element model

One beam type tested by Hassanzadeh (2006), beam type 1s, was modeled and analyzed by finite element method (FEM) using the program Diana. This beam type was chosen because freezing damage changed the failure mode from yielding of the reinforcement to bending compression failure. Both the undamaged beam and the beam exposed to freezing (internal freezing damage) were modeled and analyzed. The effect of the internal freezing damage was modeled as a change of material properties in accordance with the methodology proposed in Section 2.1.

The beam was modeled in 2D, see Figure 3. Due to symmetry only half of the beam was modeled. In

the tests, steel plates and roller bearings have been used at the supports. In the FE-model, the steel plate was modeled as infinitely stiff by constraint equations, see left end of the beam in Figure 3. The FE nodes along the plate were tied to the centre node, thus forcing the nodes to remain in a straight line, but allowing for rotation. The centre node was supported for displacement in the y -direction. Also for modeling of the loading plates on the top of the beam, the nodes were tied to remain in a straight line, see Figure 3. At the symmetry line, see right end of the beam in Figure 3, all nodes were fixed in the x -direction.

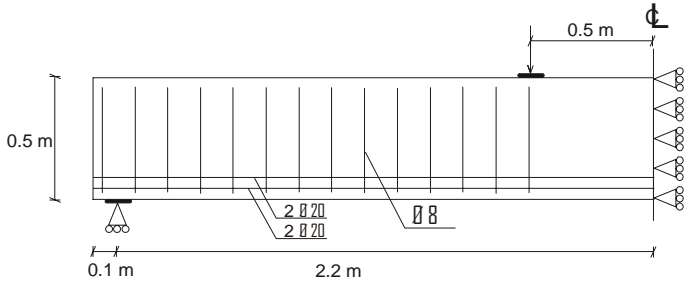


Figure 3. 2D model of half of the symmetric beam.

For the concrete, 4-node plane stress solid elements were used. The rebar layers were modeled by 2-node truss elements. To model slip between rebar and concrete, interface elements were used. The stirrups were modeled by an option called “embedded reinforcement”, corresponding to full interaction between the concrete and the steel.

The concrete was modeled with a constitutive model based on non-linear fracture mechanics using a smeared rotating crack model based on total strain; see DIANA (2006). The crack band width was assumed to be equal to the element size, 50 mm. For the tension softening, the curve by Hordijk et al. was chosen, as described in DIANA (2006). In compression, an ideal plastic behavior was used. The bond-slip relation was based on the CEB/FIP Model Code for confined concrete with good bond conditions, see CEB (1993).

Since the reinforcement type used in the experiments had not been reported in Hassanzadeh (2006), the reinforcement steel was in the finite element analyses modeled as elastic-perfect plastic and the yield stress was calibrated so that the maximum load agreed with the experimental result for the undamaged beam. The same yield stress was used for the rest of the analyses.

The material properties used in the analyses are shown in Tables 1-2. For the undamaged case, the material properties used in the analysis were based on the measured compressive strength and fracture energy in Hassanzadeh (2006) and calculated tensile strength and E-modulus using ENV 1992-1-1 EC2 and CEB-FIP Model Code 1990 respectively. For

the frost-damaged case, several analyses were run with varying material properties due to the large scatter of the measured material properties. The fracture energy in all analyses were assumed to be the same as the measured fracture energy, 163 N/m, for the damaged concrete by Hassanzadeh (2006). In FEA-damaged-1 analysis, all measured material properties were used. It should be noted that the compressive strength was recalculated from 100*200 mm cylinder to standard 150*300 mm cylinder by multiplying with a factor of 0.96 according to Ljungkrantz *et al.* (1994), and the tensile strength was obtained from measured splitting tensile strength by multiplying with a factor of 0.9 according to CEB (1993). As the E-modulus had not been measured, the calculated undamaged E-modulus was used in this case. In FEA-damaged-2 analysis, all damaged properties were calculated from measured compressive strength using relationships for undamaged concrete. In this case the tensile strength and E-modulus were calculated using ENV 1992-1-1 EC2 and CEB-FIP Model Code 1990 respectively. For FEA-damaged-3 to 5 analyses, the tensile strengths were calculated from measured compressive strength using proposed damaged tensile strength in Equation 1. Since the scatter of E-modulus reported by Fagerlund (1994) is quite high, Figure 1(b), and the reported damaged compressive strength by Hassanzadeh (2006) is rather low, the minimum reported E-modulus for FEA-damaged-3 analysis and two higher E-modulus for FEA-damaged-4 and 5 analyses were used.

Table 1. Concrete properties

	f_{cc} [MPa]	f_{ct} [MPa]	G_F [N/m]	E_c [GPa]
Undamaged	36.2	2.41	139	31.26
FEA-damaged-1	16.8	0.9	163	31.26
FEA-damaged-2	16.8	1.59	163	24.23
FEA-damaged-3	16.8	0.68	163	4.8
FEA-damaged-4	16.8	0.68	163	7.0
FEA-damaged-5	16.8	0.68	163	15.0

Table 2. Reinforcement properties

	f_y [MPa]	E_s [GPa]
Reinforcement	670	196

An incremental static analysis was performed using a Newton-Raphsson iterative scheme to solve the non-linear equilibrium equations. First, the self-weight gravity load was applied. Then, the external load was gradually applied as prescribed displacement at the loading point.

3.3 Results

The total load versus midpoint deflection graphs from the experiments and FE-analyses for both the undamaged and freezing damaged beams are shown in Figure 4. Figures 5-7 show the deformed shape and the crack distribution (in terms of maximum contour plots of the tensile strain) for both the undamaged and frost-damaged beams from the analyses. Figures 8 to 10 show the compressive stress and strain in concrete and the stress in the reinforcement versus beam deflection.

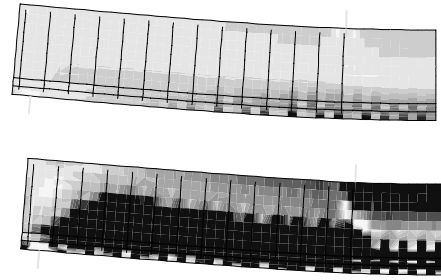


Figure 7. Deformed shape and crack development (maximum tensile strains) for frost-damaged beam before and after failure (5 and 59 mm deformation at midspan) from FEA-damaged-3 analysis.

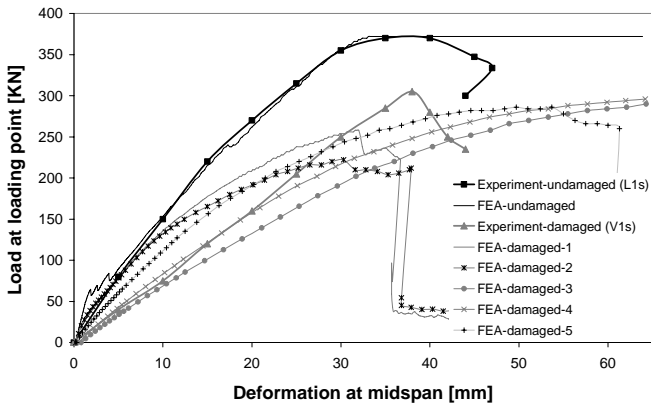


Figure 4. Load-displacement curves from analyses and experiments.

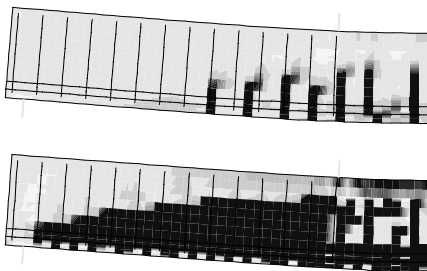


Figure 5. Deformed shape and crack development (maximum tensile strains) for undamaged beam before and after failure (5 and 59 mm deformation at midspan) from FEA-undamaged analysis.

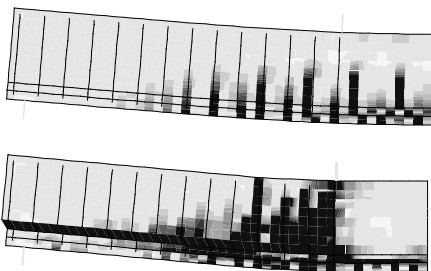


Figure 6. Deformed shape and crack development (maximum tensile strains) for frost damaged beam before and after failure (5 and 59 mm deformation at midspan) from FEA-damaged-1 analysis.

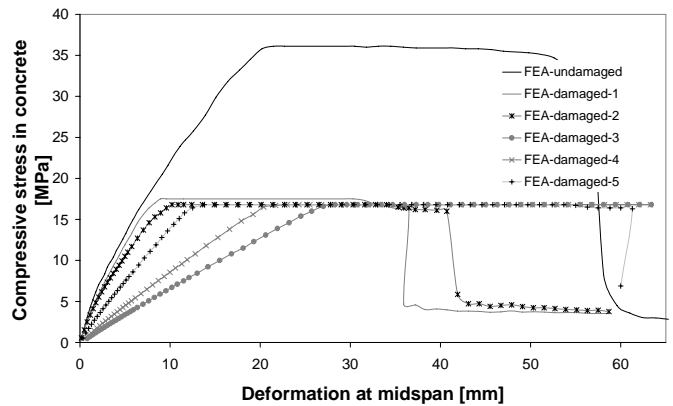


Figure 8. Compressive stress in concrete under the loading point versus beam deflection at midspan.

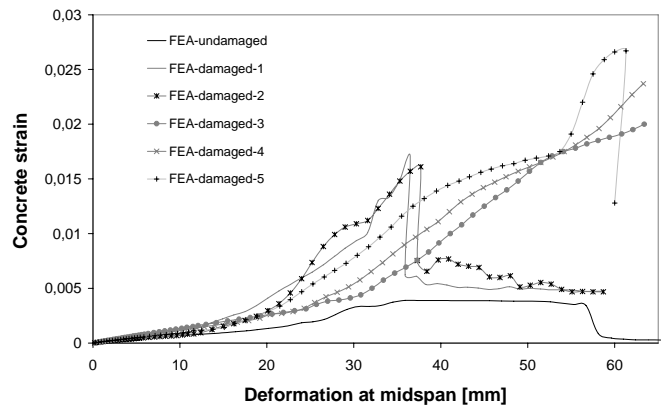


Figure 9. Strain in concrete in x -direction under the loading point versus beam deflection at midspan.

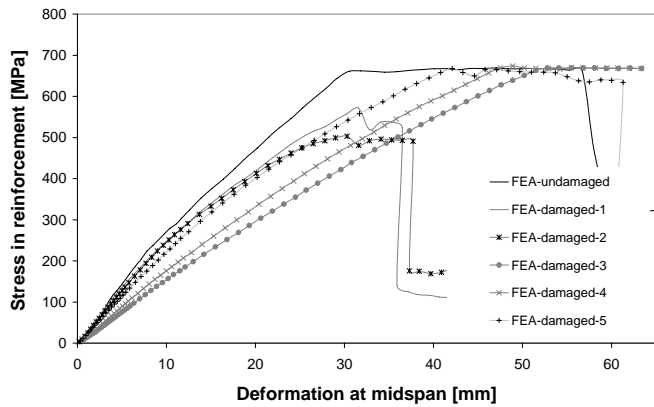


Figure 10. Stress in bottom reinforcement at midspan versus beam deflection at midspan.

The load-deflection graph shows good agreement between the analysis and test for the undamaged case, see Figure 4. For the damaged case the agreement between the test and the analyses are less good, which may depend on the large scatter of the measured material properties. The analyses of the damaged case are discussed in the following.

The analyses cases 1 and 2 are initially too stiff compared to the test, but fails at a lower load level (-15% and -30%, respectively), see Figure 4. The deformed shape and crack distribution, Figure 6, indicate that a shear failure occurred in these analyses. However, it should be noted that as an ideal plastic behavior was used for the concrete in compression, the model could not be expected to describe concrete crushing in a fully realistic way. As can be seen in Figure 8, the concrete reached its maximum capacity in compression for a load level lower than the maximum load. When examining the compressive strain in the concrete under the loading point, Figure 9, it can be seen that large strains were obtained. Thus, in these analyses, it can be concluded that the observed failure mode in shear most likely is a secondary effect caused by the limited modeling of the crushing of the concrete on the compressive side. This agrees with the failure mode reported from the test, which was concrete crushing in bending.

In the analyses cases 3 to 5 where the tensile strengths were calculated using proposed relationship in equation(1) and Young's modulus were varied, the stiffness prediction improves compared to the experiment. Case 4 gives the best agreement for the stiffness. Concerning the failure mode, the reinforcement yielded in these analyses, see Figure 10. However, it should be noted that the concrete reached its maximum capacity in compression before the reinforcement yielded, and that large compressive strains in the concrete under the loading point were obtained, Figure 10 and 9. Thus, again, most likely the analyses should not be trusted all the way to maximum load, due to the simplified modeling of concrete in compression. Hence, by varying

the Young's modulus, the stiffness could be better predicted compared to the test, but the failure load and failure mode could not be described properly.

To enable a better description of the concrete compression failure mode, it would have been necessary to include the softening of concrete in compression, and also to give a descending branch of the stress-strain curve. When this is done, localization of the deformations in a compressive failure needs to be taken into account. Van Mier (1984) showed that the compression softening behavior is related to the boundary conditions and the size of the specimen. One problem when modeling this is that the number of elements in which the compressive region will localize is not known when the analysis is started. While in tension, it seems reasonable to assume that a crack will localize in one element, an assumption that is not so obvious for compression. This complication is the reason why the simplified modeling in compression was chosen in the analyses presented here.

4 CONCLUSIONS

The paper has presented a methodology to analyze the mechanical behavior of reinforced concrete structures affected by freezing damage. The proposed methodology was tested on concrete beams affected by internal freezing damage, using non-linear FE-analyses based on fracture mechanics in the program Diana 9.1. The results of the analyses were compared with available experimental results from Hassanzadeh (2006).

The undamaged beam failed due to yielding of the bending reinforcement. As expected, good agreement between the analysis and the experiment was obtained, both regarding stiffness and strength. For the freezing damaged case, the agreement between the test and the analyses are less good, which also could have been expected due to the large scatter of the measured material properties. Therefore, several analyses were run with varying material properties. With a proper choice of the elastic modulus the stiffness of the damaged beam could be reproduced. However, the analyses gave a low failure load (in the range -5% to -30%). Further, in the experiment, the freezing-damaged beam changed failure mode to bending compression failure. This failure mode could not be predicted in a correct way in the analyses, due to the simplified modeling of concrete in compression (ideal plastic behavior was used for the concrete in compression).

Future research should focus on refinement and testing of the proposed methodology on more experimental set-ups, including a better modeling of the compressive behavior. In particular, the correlation between compressive strength and other parameters need to be examined by more tests.

REFERENCES

- CEB (1993). *CEB-FIP Model Code 1990*. Lausanne, Switzerland: Bulletin d'Information 213/214.
- DIANA (2006). *DIANA Finite Element Analysis, User's Manual, release 9.1*. TNO Building and Construction Research.
- Fagerlund, G. (2004). *A service life model for internal frost damage in concrete*. Lund: Univ.
- Fagerlund, G. & Janz, M. & Johannesson, B. (1994). *Effect of frost damage on the bond between reinforcement and concrete*. Div. of Building Materials, Lund Institute of Technology
- Gudmundsson, G. & Wallevik, O. (1999). Concrete in an aggressive environment. *Frost damage in concrete (International RILEM Workshop), Pro 25*, 1999.
- Hassanzadeh, M. & Fagerlund, G. (2006). Residual strength of the frost-damaged reinforced concrete beams. *III European Conference on Computational Mechanics Solids, Structures and Coupled Problems in Engineering*, Lisbon, Portugal, 2006.
- Neville, A.M. (2003). *Properties of concrete*. London: Pearson prentice Hall.
- Powers, T. C. (1945). A working hypothesis for further studies of frost resistance of concrete. *Journal of American Concrete institute* 16 4: 245–271.
- Shih, T.S. & Lee, G.C. & Chang, K.C. (1988). Effect of freezing cycles on bond strength of concrete. *Journal of Structural Engineering* 114 3: pp. 717-726.